EGU2020-10755
https://doi.org/10.5194/egusphere-egu2020-10755
EGU General Assembly 2020

Neogene and active brittle deformation on Amorgos Island (Greece)

Jan H. Behrmann (1,2), Jakob Schneider (2) & Benjamin Zitzow (2)

(1) GEOMAR, Wischhofstr. 1-3, 24148 Kiel, Germany; (2) IfG, Universität Kiel, Ludewig-Meyn-Str. 10, 24118 Kiel, Germany

Abstract

Amorgos is the south-eastern outpost of the Cyclades Islands in the Aegean Sea, which forms part of the Neogene-Quaternary zone of crustal and lithospheric N-S upper plate extension northward of the Hellenic subduction zone and deep sea trench. Apart from subduction-related earthquakes further south, the southern Aegean is affected by frequent earthquakes sourced in the upper plate. The twin earthquakes of 9 July 1956, followed by a strong tsunami, were the strongest events of this kind in the past Century. Hypocenters are related to a NE-SW oriented normal fault bounding the Amorgos-Santorini Graben System. There are questions in the literature regarding the seismic source and fault plane solutions, especially the contribution of a transcurrent faulting component.

We have analyzed the kinematics of brittle faults exposed on Amorgos Island itself that could be related to Neogene and active extensional and/or transcurrent deformation. Seismic slip often occurs on previously existing faults. Thus, their orientations and kinematics may help shed light on the structure of seismic sources at depth. We present evidence for a complex history of faulting. Early normal detachment faults and shear zones overprint older (rare) reverse faults, and are themselves overprinted by several sets of dominantly dextral NE and SE trending strike slip faults. Youngest is a conjugate set of NE trending high-angle normal faults. These are especially frequent along the SE coast of the island, suggesting a clear spatial relationship with the 1956 rupture. They can be fitted to a moment tensor solution similar to the published solutions for the 1956 Amorgos earthquake. The kinematic solution for the population of early normal faults suggests that the whole of Amorgos Island may have experienced a 15° NNW tilt during later extension, which lets us suspect that the island could be a tilted block of a much larger fault system. Regarding long-term late Neogene to Quaternary kinematics, dextrally transtensive fault slip is required to fit the regional pattern of extensional deformation in the Aegean, and this is reflected by small-scale brittle faulting on Amorgos.

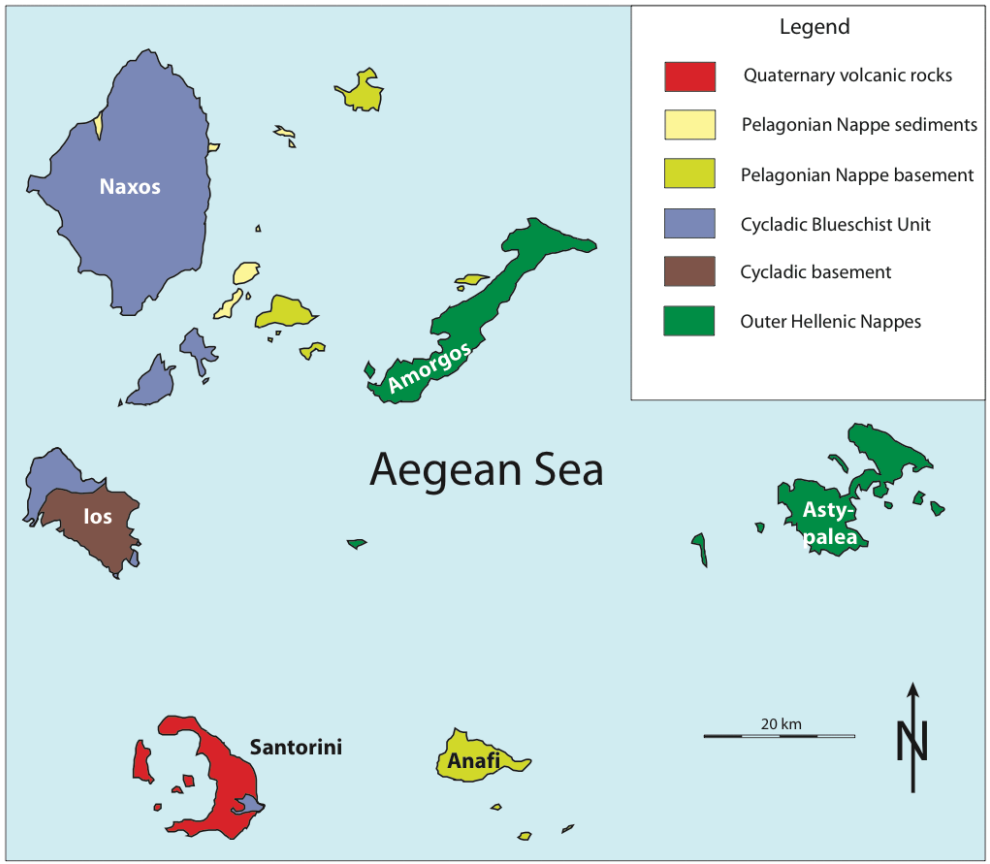

Fig. 1: Geological and tectonic sketch map of the southeast Cyclades, Aegean Sea

Geological-seismological setting

The Island of Amorgos is situated in the Greek Aegean Sea and forms part of the Southeastern Cyclades archipelago **(Fig 1)** Extensional deformation since the Miocene resulted in strong modification of the stack of Hellenic Nappes, and continues today. On July 9, 1956 the island **(Fig 2)** was struck by two earthquakes of Ms 7.4 and 7.2 - the strongest events to occur in Greece throughout the 20th Century. The offshore Amorgos Fault **(Fig 2)** broke, producing a large (30 m maximum run-up) tsunami.

(Fig. 2 on next slide)

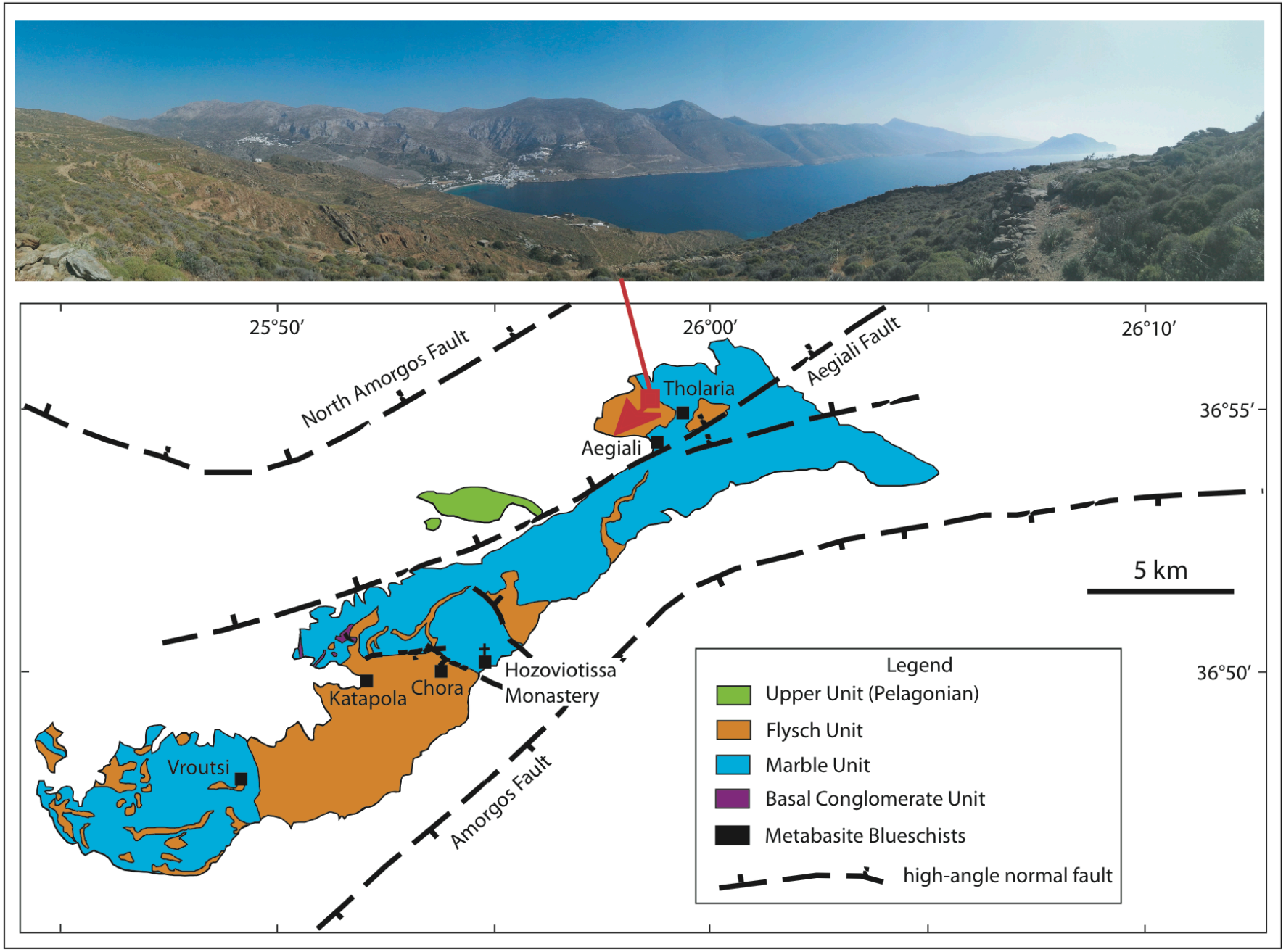

Fig. 2: Geological and tectonic sketch map of Amorgos showing the major lithological and tectonic units, major mapped and inferred fault structures, and locations mentioned in the text. After Dürr (1985), Bohnhoff et al. (2006) and Rosenbaum & Ring (2007). Vieving direction of photograph on map.

Motivation, aims, and questions

Published fault plane solutions for the earthquake are controversial **(Fig 6)**, implying the source might have a more complex geometry. Large faults **(Fig 2)** usually produce far-field deformation, and secondary faulting in damage zones. This motivated our study of brittle faulting on Amorgos. Aim was to gain insight into faulting history **(Figs 3,4)**, and the kinematics of faulting **(Fig 5)**. Finally we seek to relate the results to the rupture kinematics of the Amorgos earthquake, as derived from the seismological data **(Fig 6)**

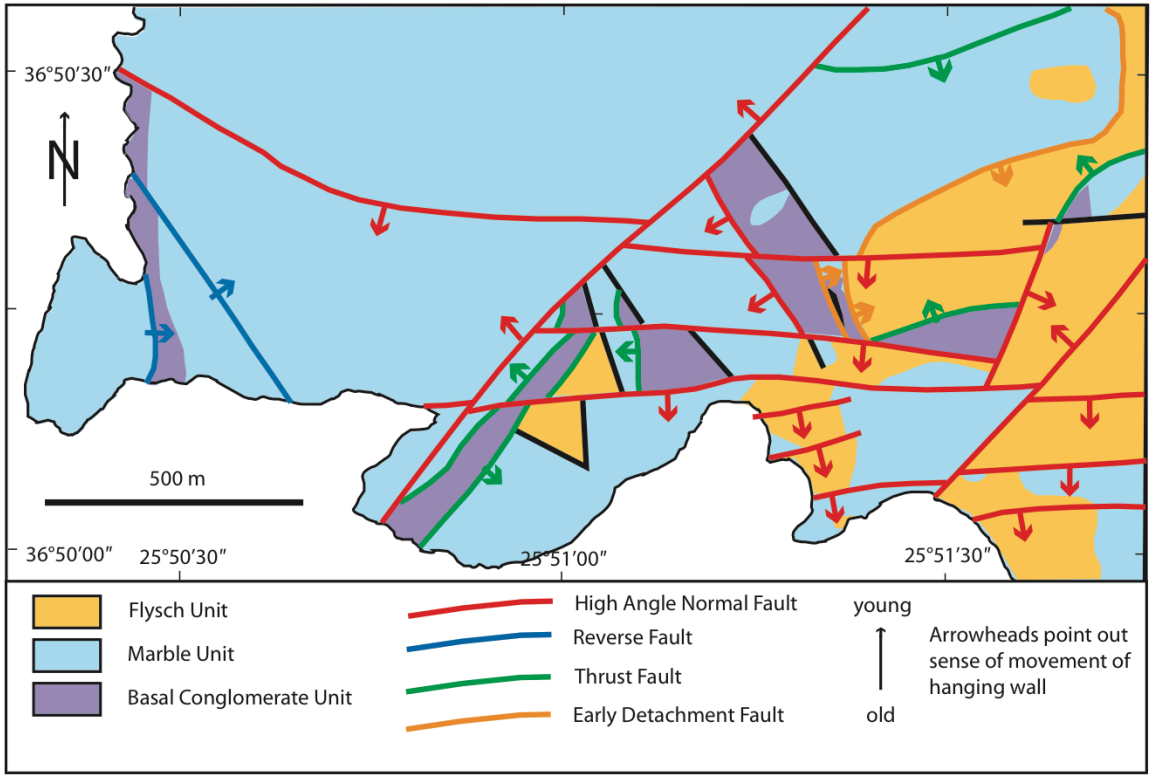

Fig. 3: Complex network of faults in the headlands WNW of Katapola **(Fig 2)**. After Rosenbaum & Ring (2007) and own field observations.

(Figs. 4-6 on following slides)

(See following and previous slides)

Fault structures and overprinting

Fault structures found in outcrops **(Fig 4)**, and the results of mapping **(Fig 3)** reveal a complex history of brittle faulting. Structures cut foliation fabrics and semi-ductile shear bands **(Fig 4b)** that were likely formed at the onset of horizontal extension of the Aegean crust in the Miocene.

The probably oldest set of brittle faults are low angle normal faults **(Figs 4e, 4f)** and detachment **(Fig 3)** structures, and are frequently found in the Katapola area **(Fig 2)** and along the central southern coast **(Fig 2)**. Sense of shear is preferentially top-SE and top-NW **(Fig 5 left)** ,suggesting subhorizontal coaxial NW-SE stretching. Reverse faulting and thrusting, mainly near the northern coast, is less frequent, and produced two weakly defined sets of conjugate faults **(Figs 3, 5 left)** The temporal relationship to older and younger normal faulting cannot be established easily, but at least the thrust faults mapped in the Katapola area **(Fig 3)** suggest phases of contractional tectonics between the two phases of brittle normal faulting.

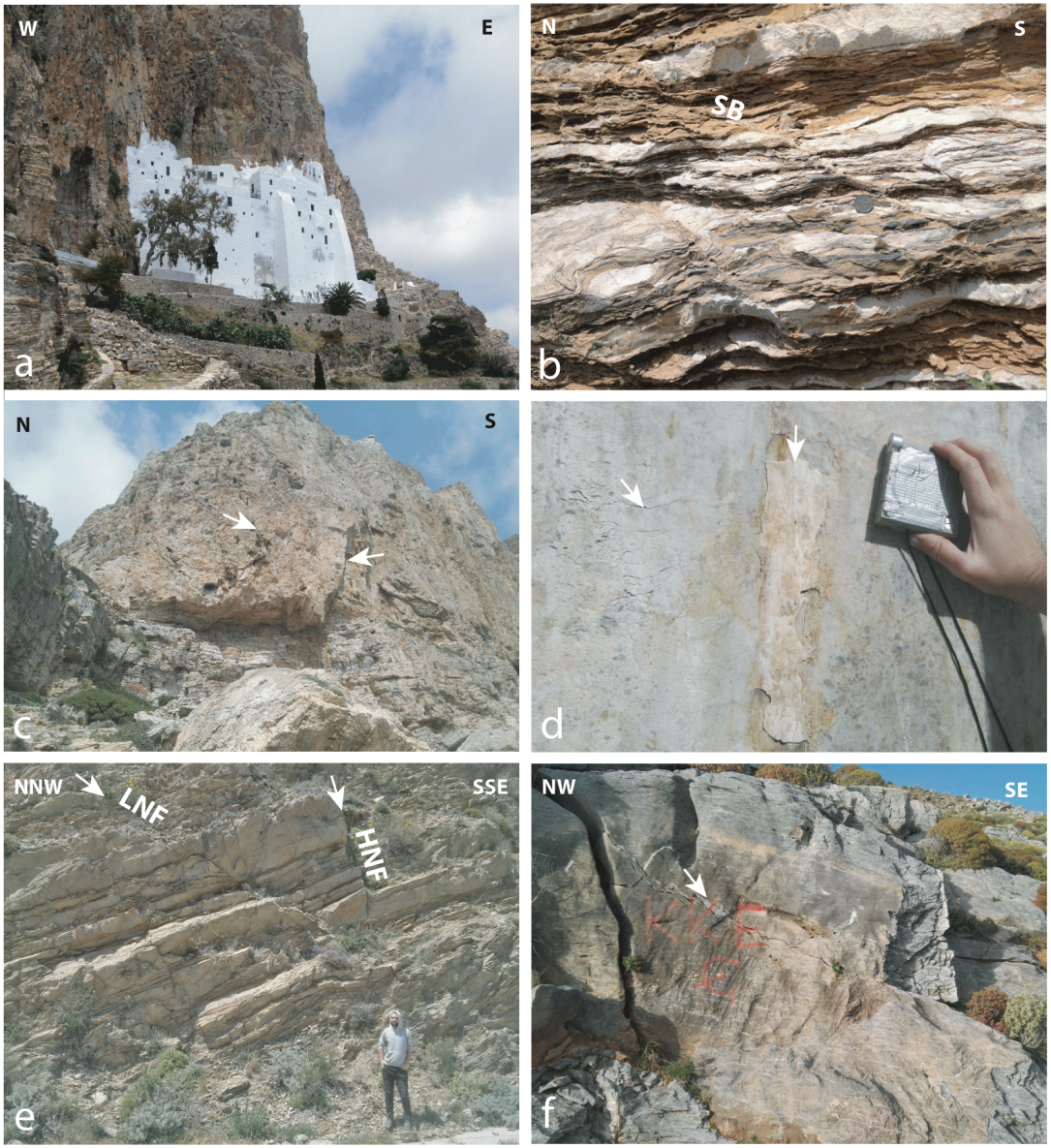

Fig. 4: Details of fault structures exposed on Amorgos.(a) Hozioviotissa Monastery **(Fig 2 for location)**, nestled in a steep SE-dipping normal fault scarp in massive marble. (b) semi-ductile shear band (SB) in thin-bedded, foliated marble, 500m WSW of the Monastery. (c) Conjugate set of steep normal faults (arrows) in massive marbles, 200 m W of the Monastery. Cliff is approx. 50 m high. (d)Polished fault plane with striae of fibrous calcite (arrow) on exposed steep normal fault. Note healed and cemented breccia and crescent-shaped steps (arrow) resulting from Riedel shears indicating normal sense of shear. (e) Low-angle normal fault (LNF) truncated by high-angle normal fault (HNF). Roadcut on route between Aegiali and Chora **(Fig 2)**. (f) Array of open en-echelon hybrid fractures in low-angle normal fault (arrow). Roadcut 1.5 km N of Chora **(Fig 2)**. Exposure is approximately 3 m high.

(See following and previous slides)

Kinematics

The whole island is dominated by high-angle normal faults of every scale **(Figs 2, 3, 4a, 4c, 4d, 4e)** forming the youngest (and probably active) phase of brittle faulting. Strike-slip faults (both, transpressive and transtensive) are variably oriented, with the majority of structures striking between NE and SE **(Fig 5 left)**. The transtensive subset of data may be kinematically and temporally connected to the high-angle normal faults, sharing a common maximum of kinematic T-axes **(Fig 5 right)**.

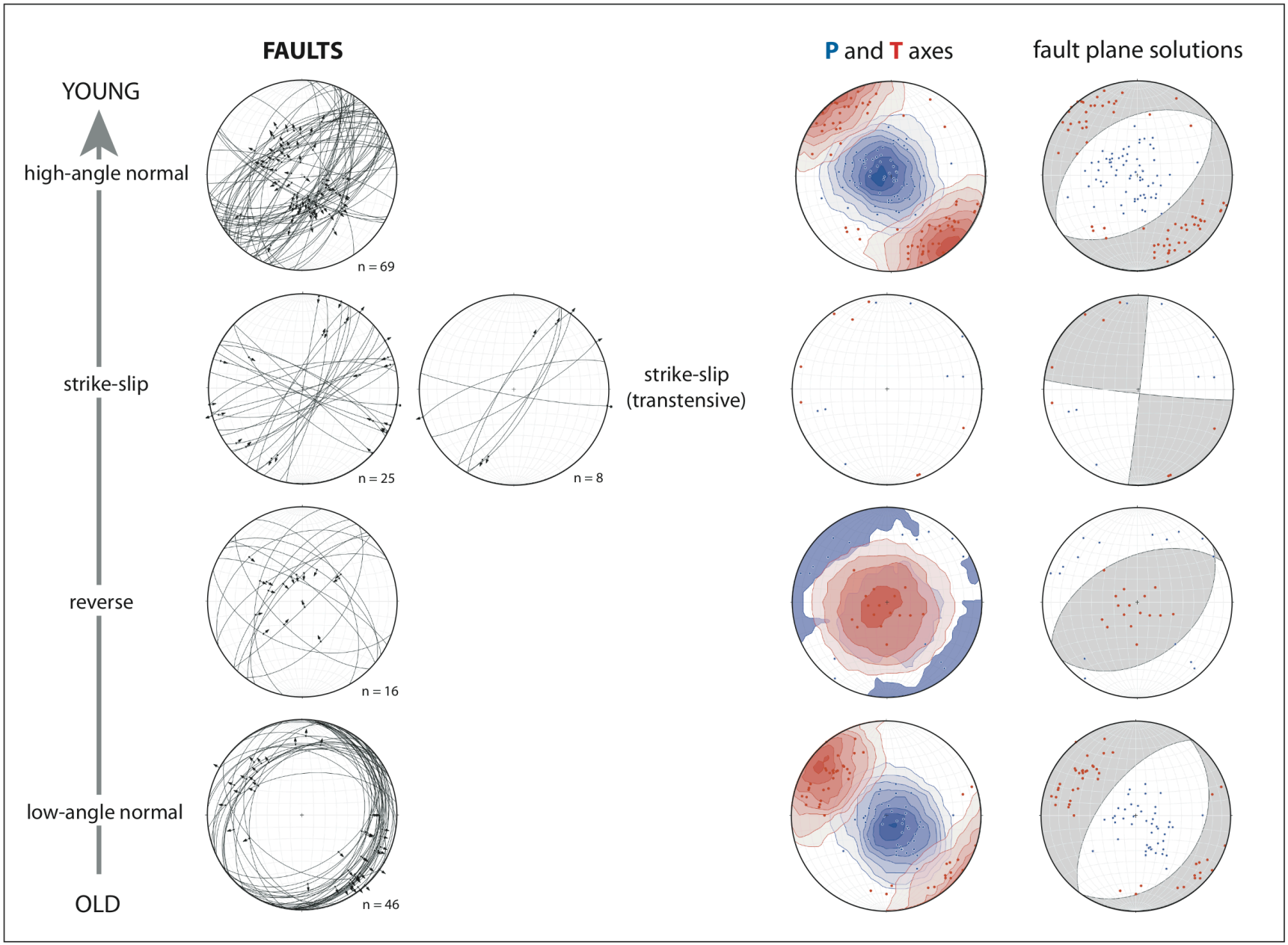

Fig. 5: Left: orientations of kinematically interpretable brittle faults found on Amorgos (whole island). Fault populations were grouped and allocated to deformation episodes on grounds of overprinting relationships **(Figs 3,4)**. Lower hemisphere, equal area projections of fault planes, associated striae and senses of hangingwall movement (arrows). Transtensive strike-slip faults were separated to show common kinematic fit with the T-axes of high-angle normal faults. Right: lower hemisphere, equal area projections of compressive (P) and extensional (T) axes distributions computed for each subset of data (partly Kamb contoured), and associated Linked Bingham fault plane solution for each subset. Computations were done using FaultKin Version 7.7.4 by R.W. Allmendinger. Algorithms of this program are described in Marrett & Allmendinger (1990).

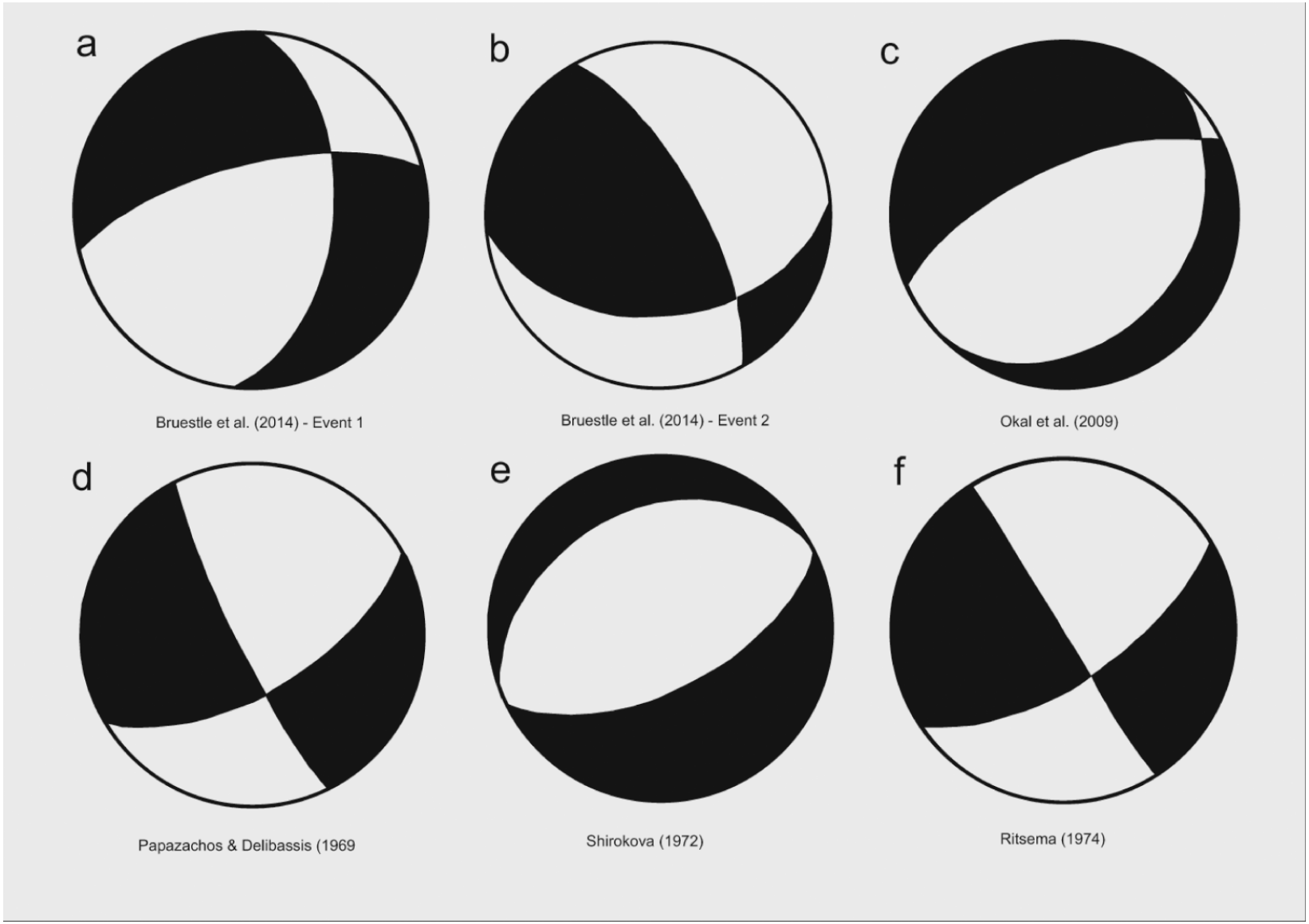

Fig. 6: All published fault plane solutions for the 9 July, 1956 Amorgos earthquake. After Papazachos & Delibassis (1969), Shirokova (1972), Ritsema (1974), Okal et al. (2009), and Bruestle et al. (2014).

(See previous slides)

Interpretation

One interesting detail concerns the kinematics of early low-angle normal faulting: the P- and T-axis maxima are tilted about 15° with respect to the vertical and the NW-SE horizontal **(Fig 5 right)**. This is a deviation from the commonly held assumption that principal stress axes are horizontal and vertical in the upper Earth´s crust, where brittle deformation dominates. We interpret this as a result of later northeastward large-scale block tilting around a NE-SW axis. Another result of this could be the geomorphic appearance of Amorgos , with relatively gentle NW slopes **(photograph in Fig 2)** and extremely rugged Alpine-style topography on the SE coast **(Fig 4a)**. The computed fault plane solutions **(Fig 5 right)** can be fitted well to the data subsets, especially in the case of the two large populations of high- and low-angle normal faults. This means that these may be related to common states of stress in the Aegean crust at the onset of brittle faulting and in the most recent geological past. The fault plane solution from high-angle normal faults fits best with the solutions proposed for the Amorgos earthquake by Shirokova (1972), and reasonably well with that by Okal et al (2009) and Event 1 of Brüstle et al. (2014) **(Fig 6)**, Suggsting a causal and kinematic relationship of young normal faulting on Amorgos and recent earthquake rupture offshore.

Conclusion

Fault slip analysis on Amorgos reveals a complex, Miocene to Recent history of faulting. The youngest high-angle normal faults are kinematically similar to the devastating 9 July 1956 earthquake and tsunami, suggesting a common stress state and attribution to NW-SE extension in the southeastern Cyclades.

References

Bohnhoff, M., Rische, M., Meier, T., Becker, D., Stavrakakis, G., Harjes, H.-P. (2006) Microseismic activity in the Hellenic Volcanic Arc, Greece, with emphasis on the seismotectonic setting of the Santorini-Amorgos zone, Tectonophysics, 423, 17–33

Brüstle, A., Friederich, W., Meier, T., Gross, C. (2014) Focal mechanism and depth of the 1956 Amorgos twin earthquakes from waveform matching of analogue seismograms. Solid Earth, 5, 1027–1044

Dürr, S. (1985) Geological Map of Greece, 1:50,000. Amorgos-Donoussa Sheet. IGME, Athens.

Marrett, R.A., Allmendinger R.W. (1990) Kinematic analyis of fault slip data, J. Struct. Geol.,12,973-986

Okal, E., Synolakis, C., Uslu, B., Kalligeris, N., and Voukouvalas,E. (2009) The 1956 earthquake and tsunami in Amorgos, Greece, Geophys. J. Int., 178, 1533–1554

Papazachos, B., Delibasis, N. (1969) Tectonic stress field and seismic faulting in the area of Greece, Tectonophysics, 7, 231–255

Ritsema, A. (1974) Earthquake mechanisms of the Balcan region, R. Neth. Meteorol. Inst., Sci. Rep., 74, 36

Rosenbaum G., Ring, U. (2007) Structure and metamorphism of Amorgos: a field excursion. Journal of the Virtual Explorer, 27(7) edited by: Lister, G.S. , Forster, M.A., Ring, U.: Inside the Aegean Metamorphic Core Complexes

Shirokova, E. (1972) Stress pattern and probable motion in the earthquake foci of the Asia-Mediterranean seismic belt, in: Elastic Strain Field of the Earth and Mechanisms of Earthquake Sources, edited by: Balakina, L. M., Vvedenskaya, A. V. , Golubeva, N. V., Misharina, L. A., and Shirokova, E. I., Nauka, Moscow